Available online at www.sciencedirect.com
SCIENCE DIRECT®
Journal of Power Sources 118 (2003) 270–275
JOURNAL OF POWER SOURCES
www.elsevier.com/locate/jpowsour

Oxygen permeation and stability of $La_{0.4}Ca_{0.6}Fe_{1-x}Co_xO_{3-\delta}$ ($x = 0$, 0.25, 0.5) membranes

S. Diethelm*, J. Van herle, P.H. Middleton[1], D. Favrat

Laboratory for Industrial Energy Systems (LENI), Swiss Federal Institute of Technology, CH-1015 Lausanne, Switzerland

Abstract

Three perovskite-type compounds of composition $La_{0.4}Ca_{0.6}Fe_{1-x}Co_xO_{3-\delta}$ ($x = 0$, 0.25 and 0.5) were investigated for use as oxygen separation membranes for the partial oxidation (POX) of methane to syngas. Special attention was given to the question of their stability in real operating conditions. A permeation set-up was specially designed to measure oxygen fluxes through these materials when placed in a strong pO_2 gradient. It also facilitated testing the long-term stability of the specimen. Permeation measurements performed in an air/argon gradient between 800 and 1000 °C showed that the highest fluxes were obtained with the highest content of cobalt ($La_{0.4}Ca_{0.6}Fe_{0.5}Co_{0.5}O_{3-\delta} \cong La_{0.4}Ca_{0.6}Fe_{0.75}Co_{0.25}O_{3-\delta} > La_{0.4}Ca_{0.6}FeO_{3-\delta}$). In addition, comparison between the fluxes of samples of different thickness gave clear evidence of surface limitations in the oxygen transport. The long-term stability test showed opposite trends: only the two lowest Co containing compounds ($x = 0$ and 0.25) sustained an air/($Ar + H_2$) gradient over more than 600 h. The other ($x = 0.5$) broke shortly after the introduction of H_2. In the presence of H_2, the oxygen flux was increased by a factor 10 compared to Ar and reached 0.83 μmol/cm^2 s for $La_{0.4}Ca_{0.6}Fe_{0.75}Co_{0.25}O_{3-\delta}$ at 900 °C. Post-operation SEM examination of the cross-section and both surfaces revealed that the surface exposed to H_2 had started to decompose resulting in the formation of a thin porous layer but the bulk of the material remained unchanged.

Keywords: Oxygen separation membrane; Permeation flux; Stability; Perovskite

1. Introduction

Over the last decade, mixed conducting perovskites have been thoroughly investigated as membrane materials for high temperature oxygen separation [1]. Such membranes can advantageously be integrated in chemical processes requiring pure oxygen [2], such as the partial oxidation (POX) of methane to synthesis gas (syngas) [3]. The production of syngas is an interesting way to valorise natural gas, since this hydrogen-rich gas mixture can be directly converted into electricity by solid oxide fuel cell (SOFC) systems. Furthermore, syngas is a major intermediate for the production of both hydrogen and gas-derived liquids, which are of growing interest for both economical and environmental reasons [4].

The constraints imposed on the materials used in oxygen separation membrane (OSM)-based POX reactors are particularly stringent. A candidate material should combine the following characteristics: (i) be a good ionic and electronic conductor; (ii) be chemically stable in both oxidising (air) and reducing (methane) conditions; (iii) be mechanically stable under operating conditions (pO_2 and temperature gradient). The two first conditions are often contradictory for the class of materials usually considered for this application [1,5], such that a compromise between high oxygen flux and stability has to be found.

A membrane under operation is subject to mechanical stresses, which mainly result from (i) mechanical constraints imposed by the reactor design (fixation, support, sealing, ...), (ii) internal stresses due to the thermal expansion of the membrane in an inhomogeneous temperature field and (iii) internal stresses due to lattice expansion of the membrane resulting from a compositional change of oxygen (chemical expansion) [6]. The latter case is probably the most critical and was identified in literature as the cause of tube fracture in POX reactors [7,8]. The mechanical and chemical stability of oxygen separation membranes materials under operating conditions, i.e. while placed in a strong pO_2 gradient between air and syngas, and delivering a significant oxygen flux, is thus an important issue.

In this study we examine the oxygen permeation and stability of three compounds of composition $La_{0.4}Ca_{0.6}Fe_{1-x}Co_xO_{3-\delta}$ ($x = 0$, 0.25 and 0.5) for application as OSM in a POX reactor. For this purpose, long-term permeation

* Corresponding author.
E-mail address: stefan.diethelm@epfl.ch (S. Diethelm).
[1] Present address: Department of Mechanical Engineering, University College London, Torrington Place, London WC1E7JE, UK.

0378-7753/03/$ – see front matter
doi:10.1016/S0378-7753(03)00098-3

measurements were performed in a strong pO_2 gradient, i.e. with air on one side and a mixture of hydrogen and argon on the other. This latter gas mixture was chosen to reproduce the harsh condition prevailing in a POX reactor (H_2 being the principal and most reducing component of syngas) instead of methane, in order to avoid the problem of the catalyst. A systematic approach was applied for the test procedure of the candidate membrane materials: (i) determination of the activation energy for the oxygen flux, from air/argon permeation measurements performed in the temperature range 800–1000 °C; (ii) long-term (500–700 h) permeation measurement at a fixed temperature (850–900 °C) with 10, 20 or 66% hydrogen mixed to the argon; (iii) post-operation scanning electron microscope (SEM) examinations of the cross-section and surfaces of the membrane, combined with energy dispersive X-ray (EDX) analysis for the detection of compositional (segregation, decomposition, ...) or morphological changes.

2. Experimental

2.1. Sample preparation

The $La_{0.4}Ca_{0.6}Fe_{1-x}Co_xO_{3-\delta}$ ($x = 0$, 0.25 and 0.5) powders were prepared following a modified citrate procedure from nitrate precursors of the metal ions, followed by calcination at 950 °C for 4 h. The phase purity was checked by X-ray powder diffraction (XRD).

The disc samples were produced by uni-axial compaction of the powder at 100 MPa and sintered in air at 1250 °C for 4 h. The density of the sintered samples was measured by the Archimedes method.

In the subsequent sections, the following abbreviations will be used: LCFC-4655 for $La_{0.4}Ca_{0.6}Fe_{0.5}Co_{0.5}O_{3-\delta}$, LCFC-463/41/4 for $La_{0.4}Ca_{0.6}Fe_{0.75}Co_{0.25}O_{3-\delta}$ and LCF-461 for $La_{0.4}Ca_{0.6}FeO_{3-\delta}$.

2.2. Permeation measurements

The permeation measurements were performed on dense ~24 mm diameter discs. The experimental set-up is sketched in Fig. 1. The discs are tightened between two open-ended alumina tubes by means of gold rings fabricated from a gold wire. This arrangement is slid into a single mullite ceramic tube that fulfils multiple functions: (i) it provides a guiding tube for positioning and securing the gold ring seals. (ii) It allows to flush the disc periphery with inert gas in order to control its contribution or loss to the permeation flux of oxygen. In addition, the disc periphery is coated with gold paste so as to minimise this contribution. (iii) It allows for the detection of leaks around the gold seals by analysing the inlet and outlet compositions of the gas flushing through this mullite tube.

The whole set-up is swagelocked with Teflon ferrules at its extremes (in the cold) and spring-loaded so as to control

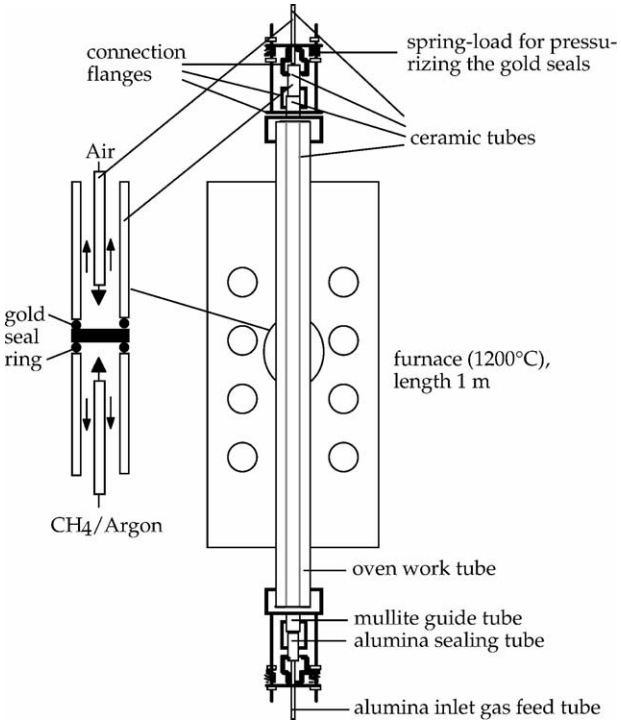

Fig. 1. Experimental set-up used for the permeation measurements.

the pressure on the gold seals, and mounted into a tiltable tubular furnace. Temperature is brought close to the melting temperature of gold (~1050 °C) in order to seal, via the pressurised gold rings, the two alumina tube chambers on either side of the membrane pellet. Then temperature can be varied down to the measurement temperature maintaining controlled tightness. Air is passed in one alumina tube, and argon (or H_2 and argon) in the other tube, in order to provide an oxygen partial pressure gradient. Oxygen permeates through the dense pellet from the air chamber to the other tube. Detailed composition analysis of the outlet gas is measured by off-line gas chromatography (*Chrompack*). The latter consists of a Molecular Sieve 5 Å with argon gas carrier, capable of detecting H_2, O_2 and N_2. Any contribution due to leakage could be corrected on the basis of the content of N_2.

3. Results and discussion

3.1. Phase development

XRD of the calcined powder for all three compositions revealed a principal cubic phase with minor secondary phases. During sintering, a second orthorhombic phase—isotypic with $Ca_2Fe_2O_5$—has developed, most clearly in the Fe-rich compositions (LCFC-463/41/4 and LCF-461). This was also observed by Stevenson et al. when synthesising Ca-rich perovskite-type compounds [9]. The amount of this second phase was estimated to 19% for LCFC-463/41/4 and 8% for LCF-461 by comparison of the intensities of the

Table 1
Atomic compositions of the different phases as evaluated from EDX

Material	La (%)	Ca (%)	Fe (%)	Co (%)	Phase fraction (%)	Composition
$La_{0.4}Ca_{0.6}Fe_{0.5}Co_{0.5}O_{3-\delta}$, LCFC-4655						
Global	11.36	12.33	12.88	10.55		$(La_{0.48}Ca_{0.52})_{1.01}Fe_{0.55}Co_{0.45}O_x$
Light phase	12.77	9.37	11.8	9.27	76.2	$(La_{0.58}Ca_{0.42})_{1.05}Fe_{0.56}Co_{0.44}O_x$
Dark phase	5.38	18.56	13.35	11.10	23.8	$(La_{0.23}Ca_{0.77})_{0.98}Fe_{0.55}Co_{0.45}O_x$
$La_{0.4}Ca_{0.6}Fe_{0.75}Co_{0.25}O_{3-\delta}$, LCFC-463/41/4						
Global	20.00	27.45	35.07	14.45		$(La_{0.42}Ca_{0.58})_{0.96}Fe_{0.71}Co_{0.29}O_x$
Light phase	23.27	24.63	35.22	13.98	75.4	$(La_{0.49}Ca_{0.51})_{0.97}Fe_{0.72}Co_{0.28}O_x$
Dark phase	10.85	36.84	34.86	14.56	24.6	$(La_{0.42}Ca_{0.58})_{0.97}Fe_{0.71}Co_{0.29}O_x$
$La_{0.4}Ca_{0.6}FeO_{3-\delta}$, LCF-461						
Global	9.92	13.44	23.02	–		$(La_{0.42}Ca_{0.58})_{1.02}Fe_{1.0}O_x$

principal peaks in the XRD pattern. In the case of LCFC-4655, no clear secondary phase could be identified from the XRD pattern. Nevertheless, the two phase texture of LCFC-4655 and LCFC-463/41/4 appeared clearly in the back-scattered electron (BSE) imaging of the sintered pellets cross-sections (Section 3.4). A representative example is given in Fig. 5, which shows a BSE picture of the air-side surface of a LCFC-463/41/4 pellet after operation. The approximate atomic compositions of each phases, as obtained from energy dispersion X-ray analysis (EDX), are displayed in Table 1. The molar fraction of each phases were calculated on the basis of their La-content with respect to the global composition. It is interesting to notice that the ratios of the transition metals (Fe, Co) remain the same in all phases. The comparison with the phase fractions determined from the XRD pattern shows reasonable agreement for LCFC-463/41/4. This means that the principal phase is probably a cubic perovskite of approximate formula LCFC-553/41/4 (light phase), whereas the secondary Ca-enriched phase would be isotypic to the brownmillerite-type $Ca_2Fe_2O_5$ (dark phase).

3.2. Oxygen flux

The oxygen permeation fluxes measured across the disc-shaped membranes for an air/argon gradient are shown in Fig. 2. The values obtained for the pure phase perovskites $La_{0.6}Sr_{0.4}Fe_{0.8}Co_{0.2}O_{3-\delta}$ (LSFC-6482) and $La_{0.6}Ca_{0.4}Fe_{0.75}Co_{0.25}O_{3-\delta}$ (LCFC-643/41/4) are also reported for comparison. As the thickness of the membrane is known to affect the oxygen flux, all fluxes were normalised to a thickness of 1 mm to facilitate the comparison. Doing so, it was assumed that the oxygen fluxes across the membranes are governed by bulk diffusion and that the hindrance related to surface reactions can be neglected. However, the limit of this assumption can be observed by comparing the fluxes corresponding to two membranes of LCFC-463/41/4 with different thickness (Fig. 3 and Table 2). The difference between the absolute and normalised fluxes, which reaches 22–47%, indicates that the oxygen flux across the membranes is partially governed by surface exchange limitations.

For an air/argon pO_2 gradient, the materials could be ranked LCFC-4655 ≅ LCFC-463/41/4 > LCF-461 for decreasing oxygen fluxes, with values comprised between 4.5 and 9×10^{-8} mol/cm^2 s at 900 °C (i.e. 40–80 l/m^2 h). These values are slightly smaller than for LSFC-6482. The apparent activation energies for the permeation fluxes can be found in Table 2.

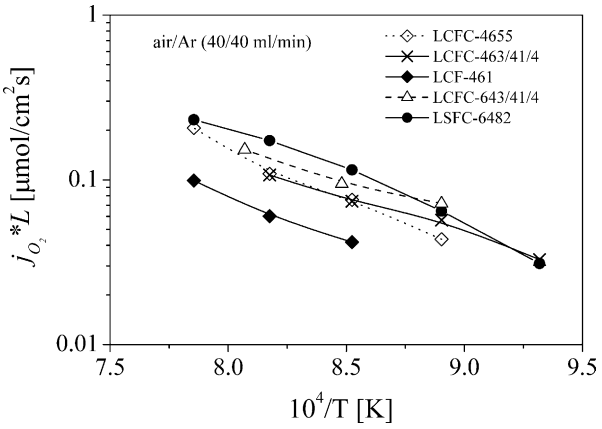

Fig. 2. Oxygen permeation fluxes corresponding to an air/argon gradient, normalised to a thickness of 1 mm. Refer to Table 1 for abbreviations.

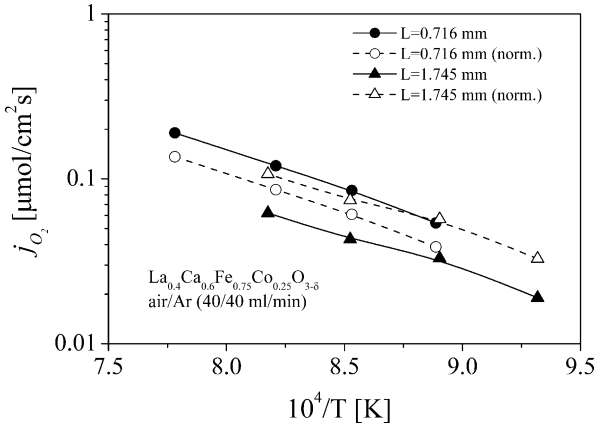

Fig. 3. Comparison between the absolute and normalised fluxes obtained for two LCFC-463/41/4 membranes of different thickness.

Table 2
Specifications of the disc-shaped membranes characterised in this work

Material	L (mm)	ρ_r (%)[a]	$Flux_{900\ ^\circ C}$ (μmol/cm^2 s)	$Flux_{900\ ^\circ C}L$ (μmol/cm^2 s)	E_A (kJ/mol)	Long-term stability in operating conditions
LCFC-4655	1.14 ± 0.01	98.7	0.066	0.075	120 ± 10	∼220 h test, cracked after introduction of H_2
LCFC-463/41/4	1.73 ± 0.02	98.3	0.043	0.074	84 ± 7	∼670 h test of which >300 h with H_2
	0.72	95.2	0.085	0.061	94 ± 3	∼720 h with H_2
LCF-461	1.02 ± 0.04	98.4	0.041	0.041	107 ± 1	>650 h test, of which >600 h with H_2
LSFC-6482	1.43	98.0	0.080	0.115	115 ± 8	–
LCFC-643/41/4	1.26	97.2	0.075	0.095	75 ± 12	–

L is the thickness of the membrane, ρ_r its relative density. $Flux_{900\ ^\circ C}$ the value of the oxygen permeation flux across the membrane at 900 °C, $Flux_{900\ ^\circ C}L$ the normalised flux, and E_A the activation energy.

[a] For two phase compounds, the theoretical density was calculated on the basis of the unit cell volume and weight of the principal phase.

Considering the two phase nature of these compounds, the significance of the measured fluxes can be questioned. However, the BSE examination of the sintered pellets (Fig. 5) shows that the secondary phase (dark phase) is restricted to isolated clusters caught in a continuous matrix of the principal phase (light phase). This suggests that the oxygen transport properties will be conferred by the latter. Comparison with the oxygen flux through the pure phase LCFC-643/41/4 perovskite further confirms this statement. As it can be seen in Fig. 2 and Table 2, the agreement with the LCFC-463/41/4 compound is satisfactory. Furthermore, those values are consistent with the flux of 0.08 μmol/cm^2 s reported in literature for LCFC-4682 at 850 °C and $L = 0.55$ mm [5]. The fluxes can thus be considered as representative of oxygen transport of the principal perovskite-type phase.

3.3. Stability of membrane materials under operating conditions

The results of the long-term stability tests under operation conditions are summarised in Table 2. Only two of the materials remained stable over a long period after the introduction of hydrogen on the oxygen-lean-side: LCFC-463/41/4, which was tested for over 700 h and LCF-461, tested for 650 h. The third material (LCFC-4655) presented important leaks shortly after the introduction of hydrogen. After cooling of the membrane, cracks could clearly be observed.

The two stability tests are shown in Fig. 4 for LCFC-463/41/4 and LCF-461. The oxygen flux was significantly increased by the introduction of hydrogen, and reached 0.83 μmol/cm^2 s for LCFC-463/41/4 at 900 °C (i.e. ∼700 l/m^2 h). This maximum value was measured shortly after the introduction of hydrogen, but the flux slowly decayed and stabilised around 0.6 μmol/cm^2 s. It should be noted that the final value was measured after a thermal cycle (900 °C → 200 °C → 900 °C), which means that the membrane successfully sustained this thermal variation.

3.4. Post-operation SEM examination

After operation in the permeation set-up, the membranes were cooled down and examined with the SEM. The cross-section and both surfaces of the membranes were analysed for micro-structural changes, and EDX analysis was performed to detect composition changes.

From the examination of the cross-sections, no compositional changes across the membranes could be detected.

The examination of the surfaces of the membranes showed that, whereas the aspect of the air-side remained unchanged (Fig. 5), the side exposed to hydrogen looked porous (Fig. 6), as if the membrane had started to decompose. Nevertheless, according to the examination of the cross-sections, this reaction is restricted to the superficial layer.

As a general trend, the surface exposed to H_2 seems to be enriched in transition metals in comparison to the average bulk composition. In particular, dark stains enriched in cobalt could be observed for LCFC-463/41/4.

In the light of those observations, we will consider the possible cause of failure of the LCFC-4655 membrane. As mentioned in the introduction, internal stresses can result from both thermal and chemical expansion of the membrane material. The first cause should be disregarded since the measurements are basically isothermal even though local production of heat due to the combustion of H_2 cannot be excluded. From literature it is known that the chemical

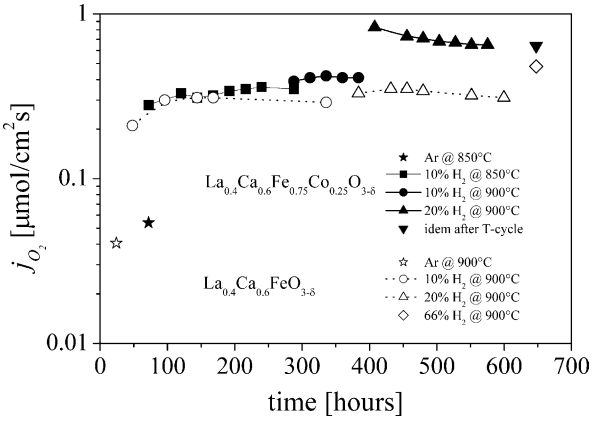

Fig. 4. Long-term stability test for LCFC-463/41/4 ($L = 0.72$ mm) and LCF-461 ($L = 1.02$ mm) membranes at 850 and 900 °C, with different oxygen lean gas compositions.

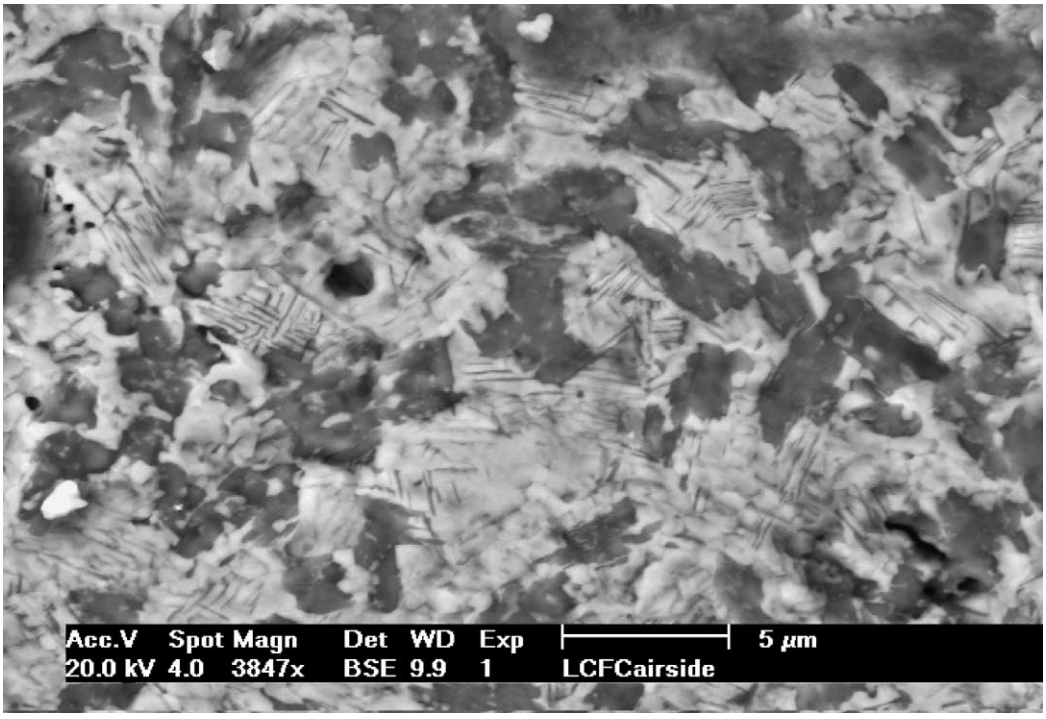

Fig. 5. BSE picture of the air-side surface of the LCFC-463/41/4 membrane after operation, showing a two-phase texture as in the bulk.

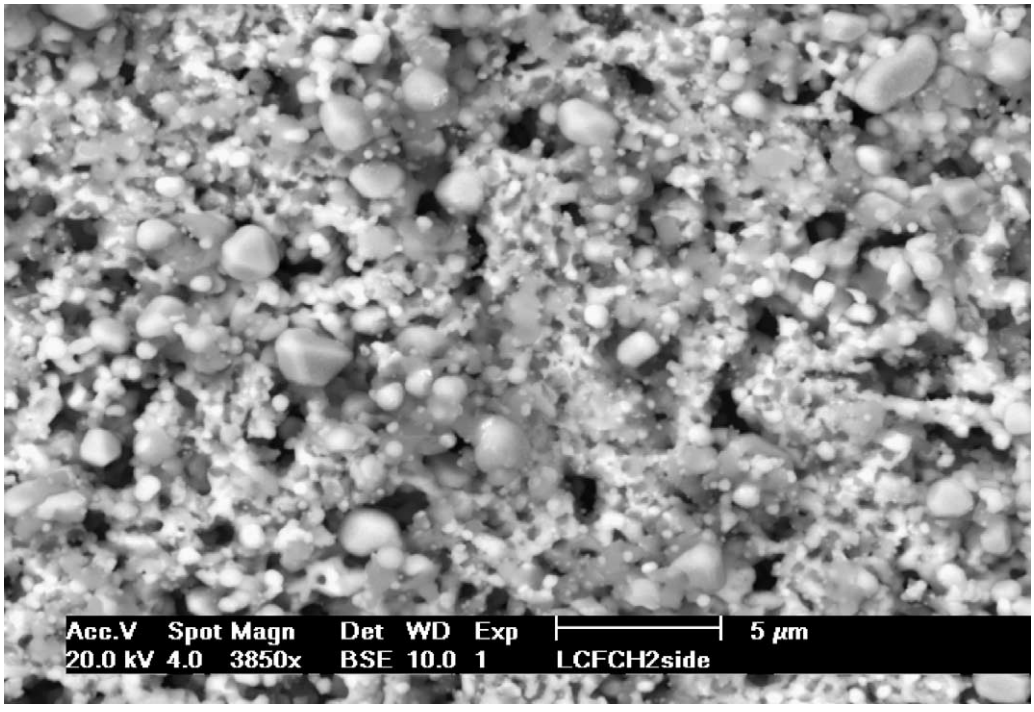

Fig. 6. Porous aspect of the surface of the LCFC-463/41/4 membrane exposed to hydrogen surface after operation.

expansion resulting from the change in oxygen stoichiometry during reduction, is increased in perovskites when Fe is substituted by Co [1]. If we consider chemical expansion as the principal cause of failure, then our results are consistent with the literature data since the Co-richest composition (LCFC-4655) is expected to be the less stable.

4. Conclusions

Three compounds of composition $La_{0.4}Ca_{0.6}Fe_{1-x}Co_xO_{3-\delta}$ ($x = 0$, 0.25 and 0.5) were tested as oxygen separation membranes in a strong oxygen partial pressure gradient. Besides a principal cubic perovskite-type phase, all three

materials presented a secondary phase enriched in Ca, isotypic with $Ca_2Fe_2O_5$. From microstructure observations, it appeared that the oxygen transport properties were conferred by the continuous perovskite-type phase.

Long-term permeation tests were performed in an air/$(H_2 + \text{argon})$ pO_2 gradient in order to check the chemical and mechanical stability of the three materials. Only the two Fe-richest compositions remained stable over 600 h with an H_2 content up to 20% on the oxygen lean side. The third composition $(x = 0.5)$, broke shortly after the introduction of H_2. This failure was attributed to the internal stresses resulting from the chemical expansion rather than from decomposition of the membrane. Post-operation SEM examinations of the membrane showed that the surface exposed to the reducing gas had started to decompose although the bulk remained unchanged.

Acknowledgements

This work was supported by the Swiss Natural Gas Union Funding (FOGA). L. Constantin from EPFL-SB-LPI, provided all powders except LCFC-643/41/4, which was produced by H.-J. Schindler at EMPA-Dübendorf, Switzerland. The XRD measurements were performed by I. Stolitchnov from EPFL-STI-LC.

References

[1] H.J.M. Bouwmeester, A.J. Burggraaf, in: P.J. Gellings, H.J.M. Bouwmeester (Eds.), The CRC Handbook of Solid State Electrochemistry, CRC Press, Boca Raton, 1997, p. 481.
[2] J.D. Wright, R.J. Copeland, Advanced Oxygen Separation Membrane, Topical report GRI-90/0303, Gas Research Institute, 1990.
[3] R. Bredesen, J. Sogge, in: Proceedings of the Paper Presentation Seminar on Ecological Applications of Innovative Membrane Technology in Chemical Industry at The United Nations Economic Commission for Europe, Chem/Sem. 21/R.12, 1–4 May 1996, Cetaro, Calabria, Italy.
[4] P.N. Dyer, R.E. Richards, S.L. Russek, D.M. Taylor, Solid State Ion. 134 (2000) 21.
[5] C.Y. Tsai, A.G. Dixon, W.R. Moser, Y.H. Ma, AIChE J. 43 (1997) 2741.
[6] P.V. Hendriksen, P.H. Larsen, M. Mogensen, F.W. Poulsen, K. Wiik, Catal. Today 56 (2000) 283.
[7] U. Balachandran, S.L. Morissette, J.J. Picciolo, J.T. Dusek, R.B. Poeppel, S. Pei, M.S. Kleefisch, R. L. Mieville, T.P. Kobylinski, C.A. Udovich, in: H.A. Thompson (Ed.), Proceedings of the Conference on International Gas Research, vol. 2, Orlando, FL, 1992, p. 2499.
[8] S. Pei, M.S. Kleefisch, T.P. Kobylinski, J. Faber, C.A. Udovich, V. Zhang-McCoy, B. Dabrowski, U. Balachandran, R.L. Mieville, R.B. Poeppel, Catal. Lett. 30 (1995) 201.
[9] J. W Stevenson, T.R. Armstrong, R.D. Carneim, L.R. Pederson, W.J. Weber, J. Electrochem. Soc. 143 (1996) 2722.